

Diffusion Kinetic Study of Chromium(VI) Biosorption by *Aeromonas caviae*

Maria X. Loukidou, Thodoris D. Karapantsios, Anastasios I. Zouboulis, and Kostas A. Matis*

Chemical Technology Division, School of Chemistry, Aristotle University, GR-54124 Thessaloniki, Greece

The removal of chromium from aqueous solution in a well-stirred batch reactor by sorption on *Aeromonas caviae* biomass particles, isolated from potable groundwater supplies, was investigated. Equilibrium and kinetic experiments were performed at various initial bulk concentrations, biomass loads, and temperatures, with promising results. It was seen that the sorption capacity is appreciable for most experimental conditions, so the biomass can be considered as a suitable biosorbent for applications. Moreover, the sorption rate of the metal ions was found to be particularly sensitive to both the initial bulk concentration and the biomass load. A detailed analysis was conducted examining several diffusion (external and intraparticle) kinetic models to identify a suitable rate expression, and interesting conclusions were reached. In this effort, information from SEM analyses and certain desorption runs was also incorporated.

Introduction

The increase of environmental contamination as a consequence of industrial development is a challenge that society must face. Heavy metal pollution usually derives from electroplating, plastics manufacturing, fertilizer manufacturing, pigments mining, and metallurgical processes. Growing attention is being paid to the health hazards presented by the existence of heavy metals in the environment; their accumulation in living tissues throughout the food chain poses a serious health problem.¹

Chromium in industrial waste, primarily present in the form of hexavalent Cr(VI) as chromate (CrO_4^{2-}) and dichromate ($\text{Cr}_2\text{O}_7^{2-}$), behaves as an oxyanion according to its aquatic chemistry.² Generally, wastewaters, such as those produced during dye and pigment production, film and photographic processing, galvanometry, metal cleaning, plating and electroplating, leatherworking, and mining, can contain undesirable amounts of chromium(VI) anions in relation to established water standards. The commonly used treatment methods for removing Cr(VI) from wastewaters include chemical precipitation, reverse osmosis, ion exchange, and membrane processes.¹ Such processes might be ineffective or extremely expensive when the initial heavy metal concentrations are in the range of 10–100 mg L⁻¹. Biosorption represents a tempting alternative technology that is based on the metal-binding capacity of various biological materials, such as algae, bacteria, fungi, and yeast, as recently demonstrated in the literature.^{3–7}

Aeromonas caviae biomass is a waste itself that is often present in groundwater and generally in aquatic environments, but little attention seems to have been given to its resistance to heavy metals.⁸ The purpose of selecting this bacterium for studying biosorption was to assess the possibility of utilizing a waste bacteria biomass for heavy metal removal, applied already effectively for a cation (Cd) removal.⁹

The biosorption of heavy metals is affected by many experimental factors such as the pH, ionic strength, biomass concentration, temperature, and presence of different metallic ions in solution. The variability of these parameters in real wastewaters makes it necessary to know their influence on biosorption performance. As a consequence of possible interactions, the comprehension of biosorption has been rather complex, requiring a study of both the heavy metal ion solution and the exact mechanism of metal uptake.^{10,11} It is known that equilibrium and kinetic analyses not only allow for the estimation of sorption capacities and rates, but also lead to suitable rate expressions characteristic of possible reaction mechanisms.

Sorption kinetics can be controlled by several independent processes that could act in series or in parallel, such as the following: (i) bulk diffusion, (ii) external mass transfer (film diffusion), (iii) chemical reaction (chemisorption), and (iv) intraparticle diffusion.¹²

For sufficiently high agitation speeds in the reaction vessel, the bulk diffusion step can be safely ignored, as then sorption onto sorbent particles is decoupled from mass transfer in the bulk mixture.

Apart from that, it is quite common that more than one process can contribute to the system performance at the same time. In this case, the extensive interrelationships among the various equations make the overall kinetic model exceedingly complicated to evaluate. A rather simplifying approach to circumvent this problem is to assume that each one of the concurrent processes dominates over the others at specific time regimes of the process (i.e., is the rate-controlling step) and, so, to study them independently.¹²

Many studies performed so far to examine sorption phenomena involved analyses of batch experiments where data were sampled at even time intervals over the entire course of the process. As a result, rapidly changing kinetic data characteristic of the phenomena occurring just after the onset of sorption could not be accurately depicted on an adequately short time scale. Thus, a primary objective of this study was to investigate the kinetic mechanism of chromium sorption on

* To whom correspondence should be addressed. Fax: 00302310997794. E-mail: kamatis@chem.auth.gr.

biomass particles with greater emphasis on samples collected at short times after the initiation of the process, when the major part of biosorption occurs.

To identify the most appropriate kinetic expression for the process, several models apparently must be checked for suitability and consistency, for a broad range of system parameters. The model selection criteria proposed by Ho et al.¹² concerning the sorption of pollutants in aqueous systems were used herein as a general guideline; several diffusion-based models were tested to describe the kinetics of metal ion uptake. The finally chosen models are those that not only fit the data closely, but also represent reasonable sorption mechanisms.

Experimental Section

Materials. *Aeromonas caviae* is a Gram-negative bacterium isolated (from filter sludge) from the potable groundwater supplies of metropolitan Thessaloniki, Greece. The cultivation medium consisted of yeast extract (0.5% w/v), tryptone (1% w/v), sodium chloride solution (0.5% w/v), and iron solution [as a dilute solution of $\text{FeSO}_4 \cdot 7\text{H}_2\text{O}$ (0.2 g L^{-1})]. The biomass was grown at 29 °C in a rotating shaker for 24 h. The produced biomass was separated by centrifugation, washed several times with a solution of NaCl (0.9%), sterilized, and then stored.

Methods. Laboratory biosorption experiments were carried out at different biomass feed concentrations (0.5, 1, and 2 g L^{-1}), initial chromium concentrations (5 and 50 mg L^{-1}), and temperatures (20, 40, and 60 °C). The batch experiments were performed in Erlenmeyer flasks at a 180 rpm agitation speed (Heidolph type, RZR 2102). This speed was selected after a number of tests at various speeds, as the lowest one that was yet good enough to give reproducible sorption curves. All biosorption experiments were carried out at the optimum pH for Cr(VI) adsorption (pH 2.5), a value also determined during preliminary experiments.⁹ Nitrate salt was selected as a possibly inhibiting anion because of its low tendency for complex formation with most metals. For the equilibrium experiments, ample contact time (2 h) was allowed. For the kinetic study of chromium adsorption, 2-mL samples were withdrawn at selected time intervals using a 10-mL syringe. Because of experimental constraints, the minimum sampling interval was 2 min.

The residual concentration of chromates in the obtained samples was chemically analyzed in solution using UV–visible spectrophotometry (Hitachi UV-200 instrument), applying a colorimetric method at 540 nm and using diphenylcarbazide.¹³ No other ions interfere with the analysis, as the reaction with diphenylcarbazide is specific for chromium(VI).

Results and Discussion

Macroscopic Observations. Optical microscopy and stereomicroscopy previously revealed that the biomass particles withdrawn from an agitated suspension were sharp-edged 3D structures with arbitrary shapes and sizes in the range of 10–100 μm . Only a few particles appeared roughly spherical, whereas many of them had faceted sides.⁹

If one considers the size of a single *A. caviae* microorganism ($\sim 0.5 \mu\text{m}$ in diameter and $\sim 2 \mu\text{m}$ in length), it is apparent that the dead biomass “particles” were

actually clusters of microorganisms brought together either by the biomass production procedure or by the shearing action occurring during agitation. In either case, this description leaves room for the hypothesis of micropores and macropores existing in the body of such clusters, an important argument regarding the possibility of intraparticle diffusion.

In an effort to investigate the surface morphology of the biomass particles, SEM imaging was also employed.⁹ Closer inspection of the largest biomass clusters showed that they had a patchy surface where smooth flakelike sections were separated by deep irregular grooves. The surface morphology of the biomass particles after the Cr(VI) ions had been sorbed (again at 20 °C) exhibited no significant difference from that prior to biosorption. This was so even though the microanalyzer of the SEM showed that the amount of sorbed Cr(VI) steadily increased as samples acquired at progressively longer sorption times were analyzed. In contrast, the gross features of the biomass at 40 and 60 °C were distinctly different from that at 20 °C. No flakes or grooves were noticeable, but instead, the surface appeared quite uneven and fragmented, with prominent ridges emerging here and there.

Equilibrium Studies. Two typical equilibrium isotherms were considered to identify the isotherm that better describes the equilibrium adsorption of metal ions onto biomass. These isotherms expressing the equilibrium metal uptake (q_{eq}) and the solution concentration at equilibrium (C_{eq}) were the following¹¹

Langmuir isotherm

$$q_{\text{eq}} = \frac{q_{\text{max}} b C_{\text{eq}}}{1 + b C_{\text{eq}}} \quad (1)$$

Freundlich isotherm

$$q_{\text{eq}} = K_{\text{F}} C_{\text{eq}}^{1/n} \quad (2)$$

where q_{max} and b , K_{F} and n are the constants corresponding to the respective isotherms.

Experimental adsorption isotherms of chromate anions, obtained with different biomass concentrations and temperatures, are presented in Figure 1a and b, respectively. For each isotherm the initial metal concentration was varied while the biomass load and temperature were kept constant. The pH value was kept constant at 2.5 for all experimental runs. The solid lines in the plots represent the best fit of the Langmuir equation to the measured data.

Table 1 reports the results of fitting the Langmuir and Freundlich models to the obtained data. Apparently, the Langmuir equation is slightly better at describing the sorption curves, as demonstrated by the higher values of the correlation coefficient (r^2). The magnitude of the maximum biosorption capacity, q_{max} , spans a range of values (from 69.95 to 284.44 mg g^{-1}) comparable to those of other types of biomass earlier reported.⁴ In addition, the values of the constant b clearly imply strong bonding of Cr(VI) to the *A. caviae* bacterial biomass at these experimental conditions. The values of the Freundlich constants indicate a relatively easy uptake of Cr(VI) anions with a high biosorptive capacity of *A. caviae*.

In summary, the adsorption isotherms obtained for Cr(VI) ion uptake by the biomass were found to follow both the Freundlich and Langmuir predictions to a

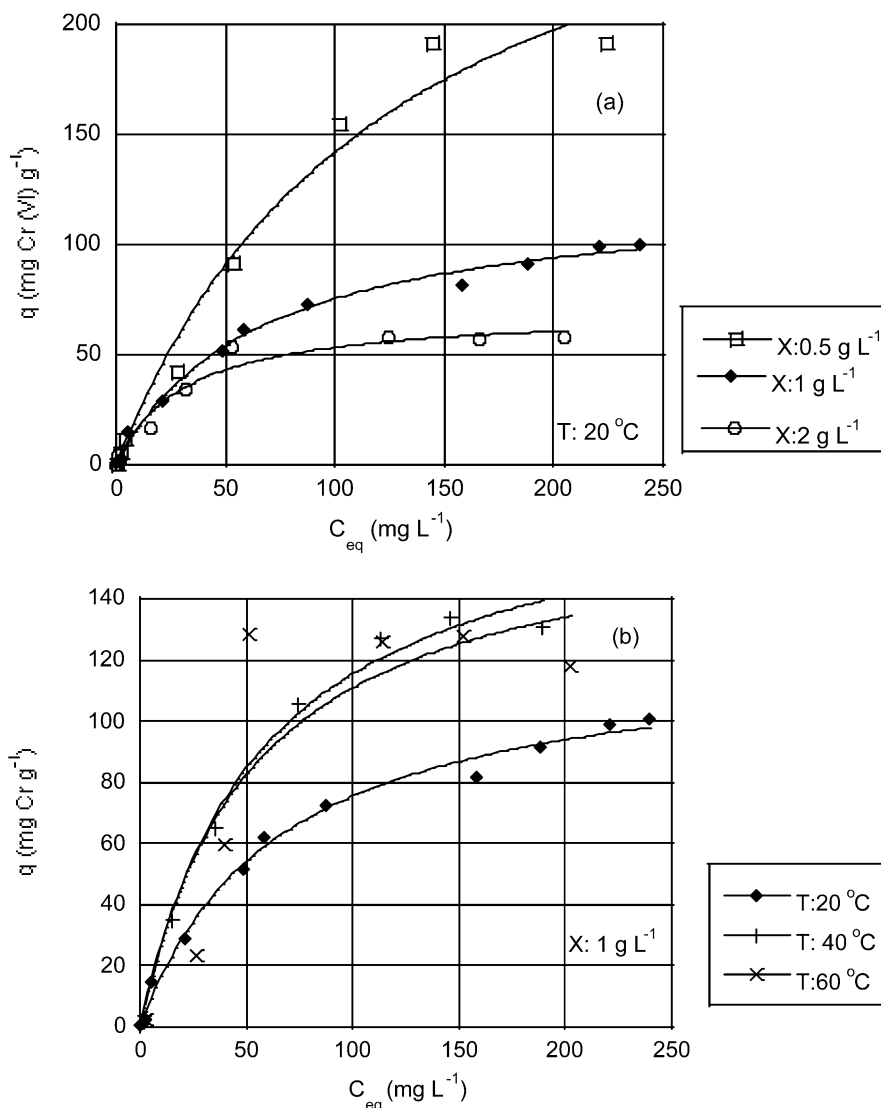


Figure 1. Equilibrium biosorption experiments of chromates at pH 2.5 for different (a) biomass concentrations, X , and (b) temperatures, T . The solid lines represent the best fit of the Langmuir model to the measured data.

Table 1. Freundlich and Langmuir Model Regression Constants for Different Experimental Conditions

conditions		Langmuir constants			Freundlich constants		
T (°C)	biomass load (g L ⁻¹)	q_{\max} (mg g ⁻¹)	b (L mg ⁻¹)	r^2	K_F (L g ⁻¹)	n	r^2
20	0.5	284.44	0.010	0.962	11.97	1.88	0.936
20	1	124.46	0.015	0.993	7.60	2.10	0.979
20	2	69.95	0.030	0.969	8.20	2.57	0.914
40	1	181.48	0.017	0.993	11.76	2.07	0.965
60	1	169.1	0.020	0.791	13.64	2.27	0.717

satisfactory extent within the studied metal concentration range (5–350 mg L⁻¹). Yet, the correlation coefficients of the Langmuir curves were distinctly higher, and the Freundlich isotherm notably suffers from the disadvantage of predicting an infinite maximum adsorption capacity, which is physically impossible.

Kinetic Experiments. Figure 2 presents the results for the concentration of chromates remaining in the bulk solution as a function of time at different experimental conditions. Unless otherwise stated, the runs were performed at 20 °C and with 1 g L⁻¹ biomass concentration. The very steep descent at the beginning of biosorption process was followed by a less rapid decay during the following 20–30 min. From that point on,

the Cr(VI) concentration declined at a much lower rate and gradually leveled off toward the end of the experiment (120 min). Thus, the major part of adsorption took place within the first 30 min of the process. The rapid kinetics has significant practical importance, as it facilitates smaller reactor volumes, thus ensuring high efficiency and economy.

As the biomass concentration rises, both the biosorption capacity, q_{\max} , and the equilibrium metal uptake, q_{eq} [i.e., the total amount of Cr(VI) ions adsorbed at equilibrium per unit mass of biosorbent], drop, manifesting a poorer biomass utilization and, hence, a low efficiency.¹⁴ Results for the latter are presented in Table 2, along with other useful equilibrium quantities. The application of different biomass (sorber) concentrations had a direct effect on the absolute metal uptake, $\Delta C (= C_0 - C_{\text{eq}})$, and the relative metal uptake, $\Lambda (= \Delta C/C_0)$. This is more obvious for the higher initial concentration. In particular, varying the biomass concentration from 0.5 to 2 mg L⁻¹ increases the absolute metal uptake by 42% for the lower initial metal concentration ($C_0 = 5$ mg L⁻¹) and by 76% for the higher metal concentration ($C_0 = 50$ mg L⁻¹). It should be stressed that the equilibrium properties do not change proportionally with the biomass load. This can be attributed to the

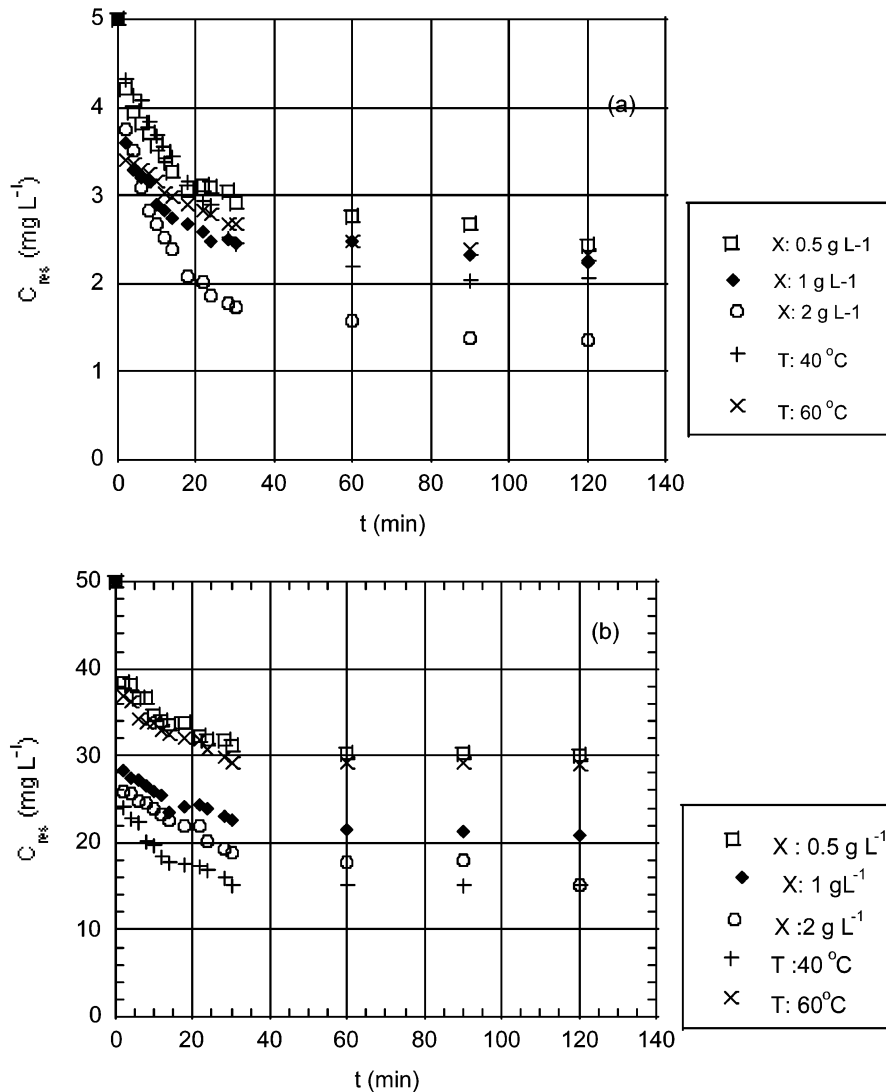


Figure 2. Chromium biosorption kinetics by *Aeromonas caviae* obtained at initial chromium concentrations (C_0) of (a) 5 and (b) 50 mg L⁻¹ (pH = 2.5, agitation speed = 180 rpm).

Table 2. Equilibrium Quantities Obtained at Different Initial Metal Concentrations, Biomass (Solid) Loads, and Temperatures

C_0 (mg L ⁻¹)	T (°C)	biomass (g L ⁻¹)	C_{eq} (mg L ⁻¹)	ΔC^a (mg L ⁻¹)	Λ^b	q_{eq} (mg g ⁻¹)
5	20	0.5	2.435	2.565	0.513	5.130
		1	2.332	2.668	0.534	2.668
	40	2	1.358	3.642	0.728	1.821
		1	2.032	2.968	0.594	2.968
	60	1	2.318	2.682	0.536	2.682
50	20	0.5	30.120	19.880	0.398	39.759
		1	21.389	28.611	0.572	28.611
	40	2	15.067	34.933	0.699	17.466
		1	15.047	34.953	0.699	34.953
	60	1	28.932	21.068	0.421	21.067

$$^a \Delta C = C_0 - C_{eq}, \quad ^b \Lambda = \Delta C / C_0.$$

possible aggregation of solids occurring at higher biomass loads, which is capable of reducing the effective adsorption area.¹⁴

The same qualitative trend is also observed upon increasing the temperature from 20 to 40 °C. However, now, the enhancement is only moderate: i.e., ~11% for $C_0 = 5$ mg L⁻¹ and ~22% for $C_0 = 50$ mg L⁻¹. A significant reduction of the metal uptake is observed at 60 °C for either bulk concentration. This latter finding

is rather unexpected and implies that direct comparison with data gathered at 60 °C might not be possible.

Beyond doubt, what is clearly inferred from Table 2 is the key role of the initial metal concentration. That is, at higher initial concentrations of Cr(VI), the adsorption capacity is markedly enhanced over and above any other parameter. Apparently, the initial concentration provides an important driving force to overcome mass-transfer resistance of Cr(VI) between the aqueous and solid phases.

Diffusion Kinetics and Modeling: Theoretical Background. To compare measurements from various experiments for the kinetics investigation, it was necessary to introduce a dimensionless degree of conversion, α . Thus, by normalizing the ion concentration remaining at time t , C_t , with respect to some reference value, an index of sorption can be defined. Taking advantage of the values of C_t before the onset of sorption, C_0 , and for completed sorption, $C_\infty = C_{eq}$, the following degree of conversion was defined

$$\alpha = \frac{C_0 - C_t}{C_0 - C_{eq}} \quad (3)$$

Intraparticle Diffusion. The solution of the diffusion equation for a time-dependent boundary condition for

the concentration at the surface of the adsorbent particle and a concentration-independent diffusivity is¹⁵

$$\alpha = 1 - 6 \sum_{n=1}^{\infty} \frac{\exp(-\xi p_n^2 t)}{9\Lambda/(1-\Lambda) + (1-\Lambda)p_n^2} \quad (4)$$

where p_n is given by the nonzero roots of

$$\tan(p_n) = \frac{3p_n}{3 + p_n^2/(1-\Lambda)} \quad (5)$$

ξ is the effective diffusional time constant, and $\Lambda \equiv (C_0 - C_\infty)/C_0$ is the relative metal uptake defined already in Table 2.

Equation 4 can be solved numerically to determine ξ , which, for the case of particle diffusion control, equals D_c/R_c^2 , where D_c and R_c are the intraparticle diffusion coefficient ($\text{m}^2 \text{s}^{-1}$) and mean particle radius (m), respectively. For Λ greater than about 0.1, the effect of a diminishing bulk concentration outside the adsorbent particle becomes significant, and under these conditions, the assumption of a constant metal concentration at the surface of the biosorbent would lead to an erroneously high apparent diffusivity.

Because our interest is chiefly focused on the short-time region ($\sqrt{D_c t}/R_c^2 < 0.2$), where eq 4 converges slowly, at least 200 terms were used in the summation to achieve satisfactory accuracy.

External Mass Transfer. An overall mass balance of the sorbate across the biosorbent surface is written as

$$Xq_t + C_t^s = C_0 \leftrightarrow q_t = \frac{(C_0 - C_t^s)}{X} \quad (6)$$

where q is the specific metal uptake (milligrams of metal per gram of biomass), C is the metal bulk concentration (mg L^{-1}), and X is the biomass fed per unit volume of solution (g L^{-1}). Subscripts o and t denote conditions at the beginning and any other instant t of the process, respectively. The superscript s denotes conditions at the biosorbent interface.

Upon combining eq 6, the Langmuir adsorption isotherm, and the equation for the rate of change in the bulk concentration, one obtains, after some algebra, the following relationships for external mass transfer¹⁶

$$\frac{dC_t}{dt} = -K_m S (C_t - C_t^s) \quad (7)$$

$$\frac{dC_t^s}{dt} = \left(\frac{K_m S}{Xq_{\max} b} \right) [(C_t - C_t^s)(1 + bC_t^s)^2] \quad (8)$$

where K_m is the external mass-transfer coefficient (m s^{-1}) and S is the specific surface area of the biosorbent particles per unit volume of the reactor ($\text{m}^2 \text{m}^{-3}$).

Using the following dimensionless variables

$$C^* = C_t/C_0, \quad C_s^* = C_t^s/C_0, \quad \text{and} \quad t^* = t\tau$$

where C_0^s has been determined from eq 6 and τ is the total adsorption time, eqs 7 and 8 can be converted to

$$\frac{dC^*}{dt^*} = -K_m S \tau (C^* - C_s^*) \quad (9)$$

$$\frac{dC_s^*}{dt^*} = \left(\frac{K_m S \tau}{Xq_{\max} b} \right) [(C^* - C_s^*)(1 + bC_s^*)^2] \quad (10)$$

which is a system of two first-order ordinary differential equations that can be solved simultaneously. The initial conditions are $C^* = 1$ and $C_s^* = 0$ at $t^* = 0$.

It must be noted, however, that normalizing C_t^s with respect to C_0^s (and not with respect to C_0 , as has been done by other authors¹⁶) and also t with respect to τ markedly improved the stability and convergence characteristics of the solution because of the comparable spreading of all variables over the computational domain.

Equations 4, 5 and 9, 10 were solved numerically to determine ξ and $K_m S$, respectively. The nonlinear numerical regression to fit experimental data to those equations was performed by the Levenberg–Marquardt method, which gradually shifts the search for the minimum of the sum of the errors squared (SSE)¹⁷

$$\text{SSE} = \sum_i \left[\frac{(q_{\text{exp},i} - q_{\text{cal},i})^2}{q_{\text{exp},i}^2} \right] \quad (11)$$

from steepest descent to quadratic minimization (Gauss–Newton).

Kinetic Modeling. Figure 3 presents the results of fitting eq 4 to biosorption data obtained at different initial concentrations, solids loads, and temperatures. It is apparent that, despite some scatter in the measurements, the finite-volume diffusion model can describe the entire range of data fairly well, including the steep concentration gradient at short times. Table 3 reports the values obtained for Λ and ξ and the computed values of D_c (for R_c set equal to $5 \mu\text{m}$).

It could be stressed that it is beyond the scope of this work to provide accurate diffusivity values, as the primary concern was to obtain a reliable rate expression equation and gain some insight into the possible mechanism of the process. That is why the calculated diffusivity values refer to the simplest case of a single microporous sorbent particle of just a representative average size. The D_c values vary within the same order of magnitude, with a clear tendency toward higher values at higher initial concentrations. Such behavior has been customarily encountered as a consequence of the decreasing slope of a nonlinear equilibrium curve, e.g., Langmuir isotherm, which causes the diffusivity to increase rapidly with increasing concentration.¹⁸

The diffusivity values shown in Table 3 lie in a realistic range of values for such systems.^{18,19} It should be mentioned that, in ref 19, the authors successfully employed the same model in studying intraparticle diffusion in the sorption of cadmium on chitosan sorbents. The diffusivity values obtained at 40 and 60 °C are below the values obtained at 20 °C for the initial metal concentration of 50 mg L^{-1} , which is opposite to what is expected physically and is ascribed to geometrical modifications of the biomass surface at higher temperatures.

A method for further investigating the possibility of a pore-diffusion-controlled mechanism is to perform desorption kinetic tests with biomass previously used for sorption. Figure 4 shows the results of such tests

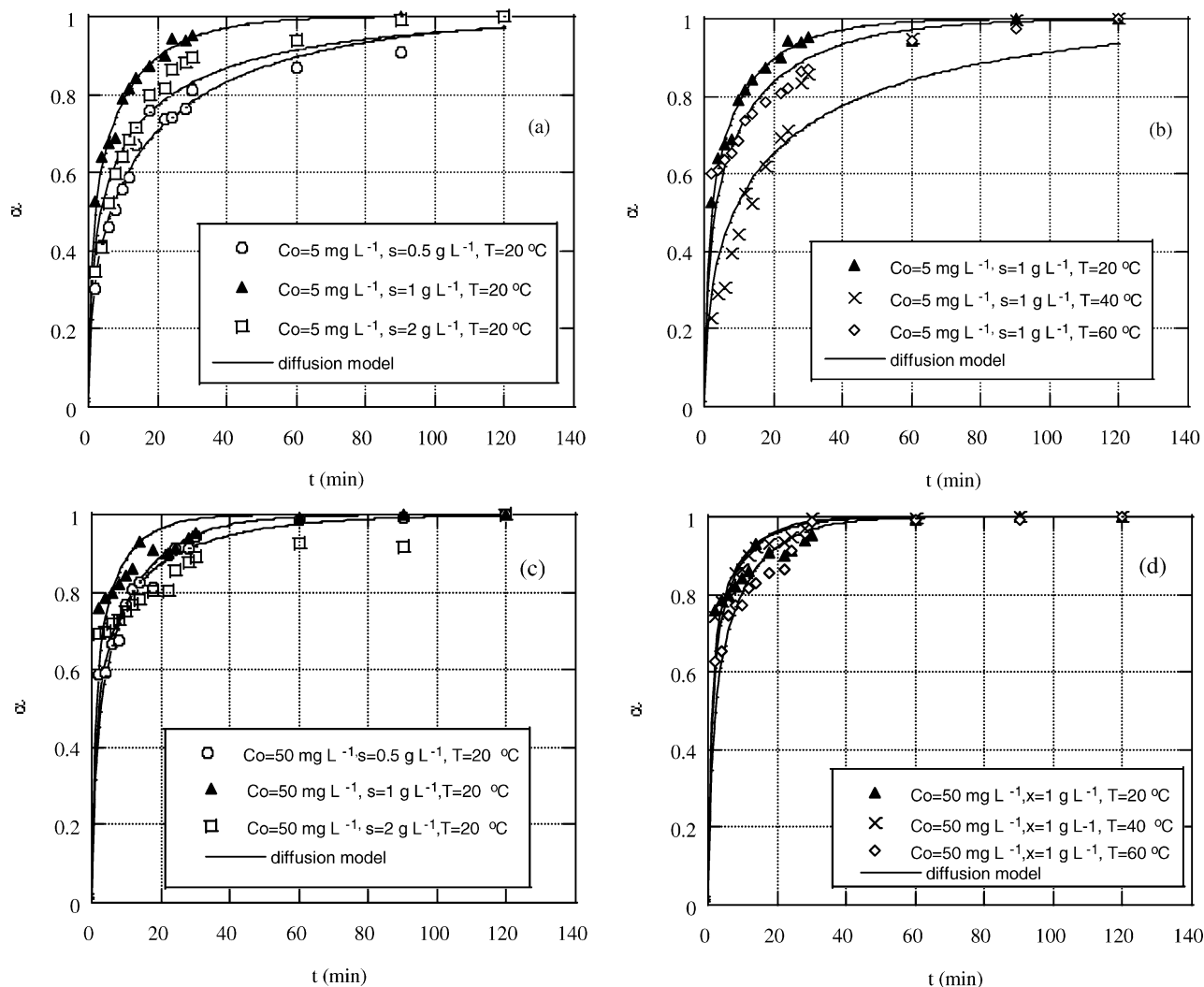


Figure 3. Experimental degree of conversion α versus predictions based on the solution of the diffusion equation (eq 4) at initial chromium concentrations of 5 mg L^{-1} for (a) various biomass loads and (b) various temperatures and 50 mg L^{-1} for (c) various biomass loads and (d) various temperatures.

Table 3. Rate Parameters Computed for Intraparticle Diffusion and External Mass Transfer Combined with Favorable Adsorption Models

C_0 (mg L^{-1})	T ($^{\circ}\text{C}$)	biomass (g L^{-1})	Λ^a	$\xi \times 10^5$ (s^{-1})	$D \times 10^{16}$ ($\text{m}^2 \text{ s}^{-1}$)	$K_m S \times 10^4$ (s^{-1})
5	20	0.5	0.513	2.6	6.4	4
	20	1	0.534	7.4	1.8	4
	20	2	0.728	1.7	4.2	6.5
	40	1	0.594	1.5	3.7	3.5
	60	1	0.536	4.9	12.4	1.6
50	20	0.5	0.398	9.1	22.8	1.5
	20	1	0.572	12.6	31.5	1.5
	20	2	0.699	3.9	9.7	1.8
	40	1	0.699	9.2	23.1	3.4
	60	1	0.421	10.9	27.3	1.5

$$^a \Lambda = \Delta C / C_0.$$

with a typical weak elution agent, Na_2SO_4 . The biomass used for desorption was originally subjected to adsorption at $20 \text{ }^{\circ}\text{C}$ at a 50 mg L^{-1} initial metal concentration and 1 g L^{-1} biomass load. For these particular conditions, the total amount of biosorbed chromium was 26.137 mg L^{-1} . As can be seen, desorption was not instantaneous, despite the particularly favorable conditions, and this can be attributed, at least in part, to the back-diffusion of a portion of the metal that was originally sorbed on internal sites of the porous biomass.

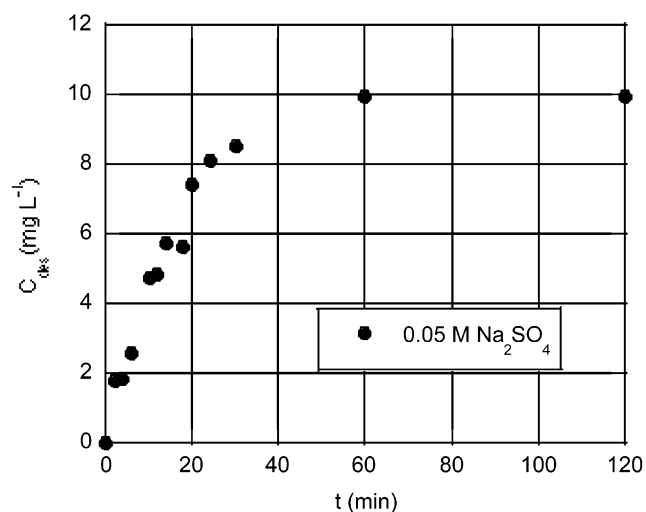


Figure 4. Chromium desorption: effect of different desorption agent; C_{des} is the desorbed concentration of chromium (conditions: $C_{\text{eq}} = 26.137 \text{ mg L}^{-1}$, biomass load = 1 g L^{-1} , pH = natural).

For the case of a nonporous biomass particle, transport of solute inside the particle can be neglected, and it can be assumed that biosorption occurs mainly at the particle surface, i.e., the cell wall. This idea can be

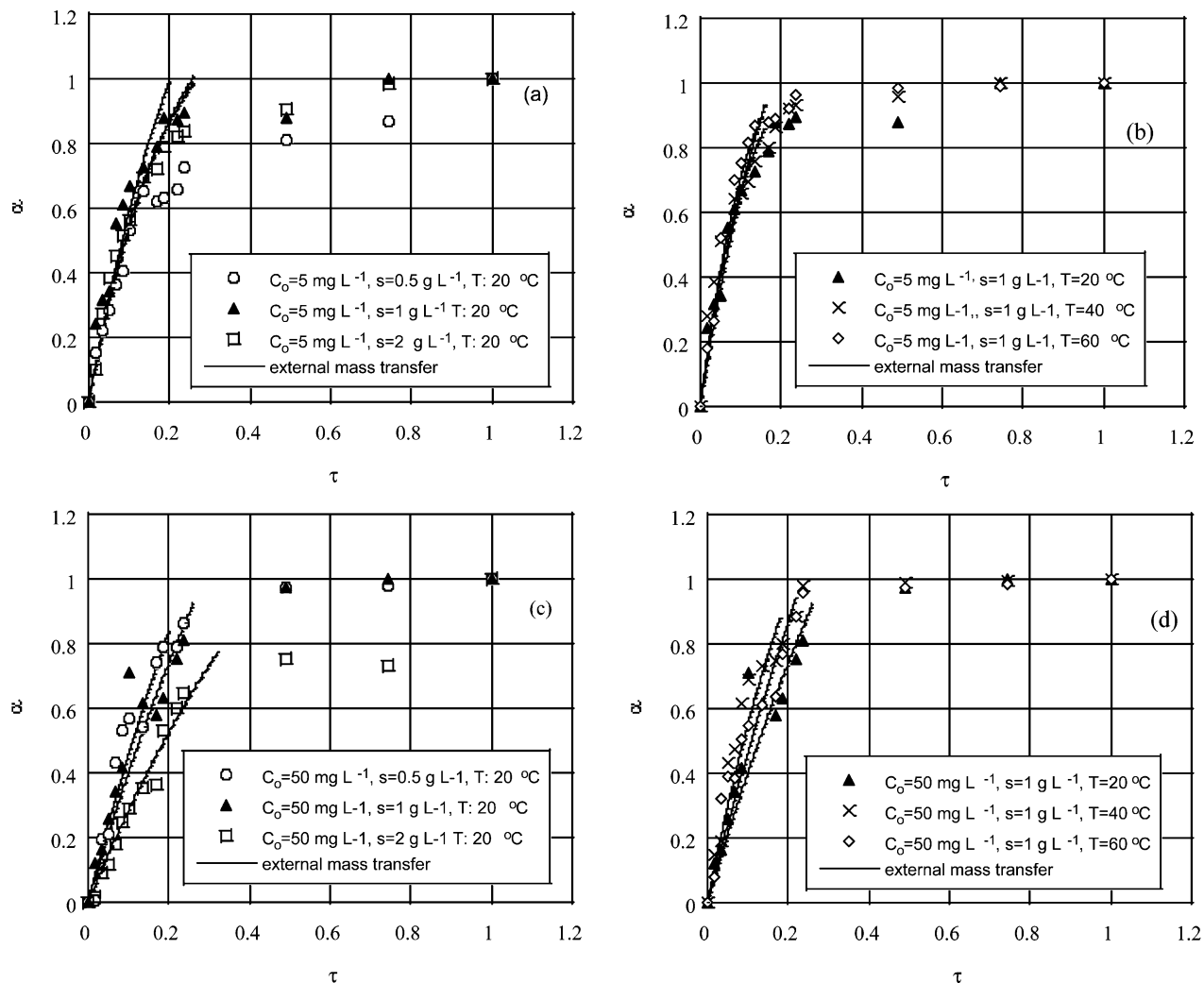


Figure 5. Experimental degree of conversion, α , with total adsorption time, τ , versus predictions based on the solution of the mass transfer equation (eqs 9 and 10) at initial chromium concentrations of 5 mg L^{-1} for (a) various biomass loads and (b) various temperatures and 50 mg L^{-1} for (c) various biomass loads and (d) various temperatures.

effectively extended to cases of relatively large macropores, where the chromium ions have ready access to react with internal surface sites.

The preliminary effort to fit eqs 9 and 10 to the entire time records of the acquired sorption data led to poor results; the prompt removal of chromium just at the onset of sorption was chiefly blamed for this problem. Such a steep concentration gradient at the initial removal stage can be tentatively explained if one considers a solid ion-exchange surface. This involves chromium molecules being instantaneously sorbed on the biomass surface, where initially there are no other such molecules and consequently adsorbate–adsorbate interactions are negligible, leading to the formation of a monolayer. The Langmuir isotherm obtained during the equilibrium study lends further support to the notion of a monolayer.

As soon as the monolayer reaches saturation, a process of spatial rearrangement of the molecules can start, yielding a further increase in the number of chromium molecules adsorbed but at a reduced rate. This second step might well be an external film-diffusion-controlled phenomenon. This is so because, when suspended particles move at a speed comparable to that of the agitated (carrier) liquid, the boundary layer around the particles usually is not completely suppressed.

Consequently, one can argue that, at the beginning of the process, chromium is sorbed according to a quite rapid and highly favorable chemical mechanism, such as the one described above, but soon external film diffusion comes into play. On this account, if one ignores the very first minute of sorption, the remaining curves were fitted pretty well by model eqs 9 and 10. Figure 5 displays these results. Near the end of sorption (for α higher than 0.9), a much slower process, e.g., intraparticle diffusion, becomes gradually the rate-controlling step. Yet, this is a regime of no practical significance.

Table 3 presents the values computed for the mass-transfer rate constant, $K_m S$. As regards the effect of changing the solids load, it appears that $K_m S$ is essentially not affected. To assess the statistical significance of the determination, a derivative time series analysis was performed in which $d\alpha/dt$ was plotted against t and then a Hanning low-pass filter was applied to flatten the signal undulations until $d\alpha/dt$ versus α became a reasonably smooth curve (local maxima below 1% of average α).²⁰ Next, the integrated smoothed signal $\alpha(t)$ was processed as before, resulting in $K_m S$ values between 1.5×10^{-4} and $6.5 \times 10^{-4} \text{ s}^{-1}$, with no preferential trend with respect to biomass load. This is an additional positive sign that external mass transfer might be the predominant mechanism of the sorption process after the initial fast chromium removal.

Conclusion

The sorption rate of chromates onto *Aeromonas caviae* particles was particularly sensitive to the initial bulk concentration and solid load. The obtained favorable biosorption results, in terms of capacity and rate, of the examined metal ion onto the biomass demonstrate a potential for technological treatment of metal waste streams by such an inexpensive waste material (suitable both for cations and oxyanions).

In the second part of this study, a kinetic investigation was conducted, involving analysis of various kinetic rate expressions mechanisms. Strong evidence was provided that the sorption of chromium(VI) onto *Aeromonas caviae* is a complex process. A finite-volume diffusion model with a time-dependent concentration at the surface of the biosorbent was found to closely fit the experimental data for the largest part of the process. Alternatively, the scenario of an external surface chemical enhancement, dominating the very beginning of the process, followed by external film diffusion was also found to meet the fitting requirements and, hence, deserves attention on physical grounds.

In view of the above, we are tempted to argue that biosorption of chromium is perhaps more correctly described by more than one model, as it often the case with the sorption of metal ions.¹⁸ This is perhaps contrary to the customary approach in the literature, where authors select just one kinetic model and, when it shows a satisfactory fit with the experimental data (based on a correlation coefficient analysis), then often readily accept the model.¹² In this sense, it is hoped that the present work constitutes an important contribution to the field, underlying the need for testing several theoretical models before making definitive statements about the process mechanism(s).

Acknowledgment

Many thanks are due to Dr. John M. Tobin (School of Biological Sciences, Dublin City University, Dublin, Ireland) for his help with the microbiological identification of the microorganism used.

Nomenclature

b = Langmuir constant ($L\ mg^{-1}$)
 C = metal bulk concentration ($mg\ L^{-1}$)
 D_c = intraparticle diffusion coefficient ($m^2\ s^{-1}$)
 K_F = Freundlich constant [$mg\ [g\ (mg\ L^{-1})^{-1/n}]^{-1}$]
 K_m = external mass-transfer coefficient ($m\ s^{-1}$)
 n = Freundlich constant
 q = specific metal uptake ($mg\ g^{-1}$)
 q_{max} = Langmuir constant ($mg\ g^{-1}$)
 R_c = mean particle radius (m)
 S = specific surface area of biosorbent per unit volume of reactor ($m^2\ m^{-3}$)
 T = temperature ($^{\circ}C$)
 t = time (min)
 X = biomass loading per unit volume of solution ($g\ L^{-1}$)

Greek Letters

α = degree of conversion

Λ = fraction of metal ultimately sorbed by the sorbent

ξ = numerically determined parameter

Literature Cited

- (1) Patterson, J. W. *Industrial Wastewater Treatment Technology*; Butterworth Publishers: Stoneham, MA, 1985.
- (2) Aksu, Z.; Sag, Y.; Kutsal, T. A comparative study of the adsorption of chromium(VI) ions to *C. vulgaris* and *Z. ramigera*. *Environ. Technol.* **1990**, *11*, 33.
- (3) Kratochvil, D.; Volesky, B. Advances in the biosorption of heavy metals. *Trends Biotechnol.* **1998**, *16*, 291.
- (4) Veglio, F.; Beolcini, F. Removal of metals by biosorption: A review. *Hydrometallurgy* **1997**, *44*, 301.
- (5) Butter, T. J.; Evison, L. M.; Hancock, I. C.; Holland, F. C.; Matis, K. A.; Philipson, A.; Sheikh, A. I.; Zouboulis, A. I. The removal and recovery of cadmium from dilute aqueous solutions by biosorption and electrolysis at laboratory scale. *Water Res.* **1998**, *32*, 400.
- (6) Volesky, B. Detoxification of metal-bearing effluents: Biosorption for the next century. *Hydrometallurgy* **2001**, *59*, 203.
- (7) Zouboulis, A. I.; Loukidou, M. X.; Matis, K. A. Biosorption of toxic metals from aqueous solutions by bacteria strains isolated from metal-polluted soils. *Process Biochem.*, in press.
- (8) Miranda, C. D.; Castillo, G. Resistance to antibiotic and heavy metals of motile aeromonads from Chilean freshwater. *Sci. Total Environ.* **1998**, *224*, 167.
- (9) (a) Loukidou, M. X.; Matis, K. A. Removal of toxic metals from dilute aqueous solutions by the application of biosorption. Presented at the VI International Conference on Protection & Restoration of the Environment, Skiathos, Greece, Jul 1–5, 2002. (b) Loukidou, M. X.; Karapantsios, T. D.; Zouboulis, A. I.; Matis, K. A. Cadmium(II) biosorption by *Aeromonas caviae*: Kinetic modelling. Presented at the 15th International Biohydrometallurgy Symposium, Athens, Greece, Sep 14–19, 2003.
- (10) Volesky, B.; Holan, Z. R. Biosorption of heavy metals. *Biotechnol. Prog.* **1995**, *11*, 230.
- (11) Yiacoymi, S.; Tien, C. *Kinetics of Metal Ion Adsorption from Aqueous Solutions*; Kluwer Academic Publishers: Boston, 1995.
- (12) Ho, Y. S.; Ng, J. C. Y.; McKay, G. Kinetics of pollutant sorption by biosorbents: review. *Sep. Purif. Methods* **2000**, *29*, 189.
- (13) *Standard Methods for the Examination of Water and Wastewater*; American Public Health Association (APHA): Washington, DC, 1995.
- (14) Esposito, A.; Pagnanelli, F.; Lodi, A.; Solisio, C.; Veglio, F. Biosorption of heavy metals by *Sphaerotilus natans*: An equilibrium study at different pH and biomass concentration. *Hydrometallurgy* **2001**, *60*, 129.
- (15) Crank, J. *Mathematics of Diffusion*; Oxford University Press: London, 1975.
- (16) Puranik, P. R.; Modak, J. M.; Paknikar, K. M. A comparative study of the mass transfer kinetics of metal biosorption by microbial biomass. *Hydrometallurgy* **1999**, *52*, 189.
- (17) Bates, D. M.; Watts, D. G. *Nonlinear Regression Analysis and Its Applications*; Wiley: New York, 1988.
- (18) Smith, E. H. Uptake of heavy metals in batch systems by a recycled iron-bearing material. *Water Res.* **1996**, *30*, 2424.
- (19) Dzul Erosa, M. S.; Saucedo, T. I.; Navarro Mendoza, R.; Avila Rodriguez, M.; Guibal, E. Cadmium sorption on chitosan sorbents: Kinetic and equilibrium studies. *Hydrometallurgy* **2001**, *61*, 157.
- (20) Bendar, J. S.; Piersol, A. G. *Random Data: Analysis and Measurement Procedures*; Wiley: New York, 1986.

Received for review September 17, 2003

Revised manuscript received January 16, 2004

Accepted January 16, 2004

IE034132N